Electronic structure, thermal, and elastic properties of Al-Li random alloys

P. A. Korzhavyi, A. V. Ruban, S. I. Simak, and Yu. Kh. Vekilov
Chair of Theoretical Physics, Moscow Institute of Steel and Alloys, Leninsky Prospekt 4, Moscow 117936, Russia
(Received 2 November 1993)

We present the results of the LMTO-CPA-LDA calculations of the electronic structure and thermodynamic properties of random Al-Li alloys. In order to take into account the charge-transfer and local-environment effects, we use a simple and physically transparent model for the Madelung potential and energy in the single-site coherent-potential approximation. As a result, all calculated ground-state properties are in good agreement with experimental data. The use of the high-temperature relation between Poisson's ratio and the Grüneisen constant allows us to calculate the thermal and elastic properties of random Al-Li alloys without any adjustable parameters on the basis of the binding-energy curves at 0 K.

I. INTRODUCTION

Despite the fact that both elements aluminum and lithium are quite normal metals, their alloys manifest rather unusual thermodynamic and electrochemical properties[1–3] which have lately prompted a number of theoretical studies of the Al-Li system.[4–15] The most surprising properties among them are the drastic increase of Young's modulus and the lattice parameter contraction of aluminum-based Al-Li alloys though Young's modulus of lithium (5–10 GPa) is almost an order of magnitude smaller than that of aluminum (66 GPa) and the atomic radius of lithium (1.55 Å) is appreciably greater than that of aluminum (1.43 Å).

To clear up the origin of the anomalous behavior of Al-rich solid solutions and its connection with the characteristic features of an interatomic interaction, several independent groups of authors almost simultaneously carried out the first-principles calculations of the electronic structure and cohesive properties of Al-Li alloys.[7–14] Among them only one work[14] deals directly with random Al-Li alloys and the others examine various ordered aluminum-rich Al-Li compounds. In the latter case, contemporary band structure methods allow one to obtain a distinct picture of the interatomic interaction and thermodynamic properties of elements and compounds with the use of only the common local-density approximation (LDA). Nevertheless, the results of Ref. 7 concerning the Al-Li system are very doubtful because the authors overlooked the d component in the wave function radial part expansion inside the lithium atomic sphere and, therefore, their results for the bulk modulus and the lattice parameter contradict the available experimental data.[2,3] In Ref. 12 the electronic structure and thermodynamic properties of the Al_3Li compound were calculated by means of the linear-muffin-tin-orbital (LMTO) method and on the basis of the analysis of the local and partial decomposition of the density of electron states the authors came to the conclusion that Al and Li atoms form a covalentlike bond due to the strong hybridization between their p and s electrons. The cause of the latter, in the authors' opinion, is due to the absence of p and d electron states in the core of lithium, which allows the states of this symmetry to form easily in the lithium atomic sphere. The authors of Ref. 9 came to a similar conclusion on the basis of more elaborate calculations within the framework of the more sophisticated full-potential linear augmented plane wave (FLAPW) method. They showed that the valence electrons of lithium promote the formation of more directional Al-Al bonding in the Al_3Li compound (having $L1_2$ structure) in comparison with pure aluminum.

Another explanation of the shear and Young's moduli growth in Al-Li alloys was proposed in Ref. 14 on the basis of the first-principles pseudopotential calculations of random Al-Li alloys within the virtual crystal approximation (VCA). According to their results, the alloying of aluminum by lithium leads to the enhancement of a singularity in the density of electron states (DOS) which lies near the Fermi energy and coincides with it at approximately 5-at.% Li. This proximity of the Fermi energy to the acute minimum point in the DOS results in the steep rise of the shear and Young's moduli of Al-Li alloys at about 5 at.% of Li, at which point both moduli reach their maximal values. Thus, the authors explain the unusual concentration dependencies of the moduli by the "band structure effects." Unfortunately, the use of the VCA makes it impossible to obtain a clearer picture of the interatomic interaction. Moreover, this approximation is too crude for the Al-Li system because it actually does not take into account the effects of charge transfer which, as will be shown below, are not negligible in this system.

In this paper, we present the results of more accurate calculations of the electronic structure and thermodynamic properties of random Al-Li alloys which have been obtained by the recently elaborated LMTO method in the coherent potential approximation (LMTO-CPA).[16,17] The most doubtful approximation, especially for the Al-Li system, in our calculations is the single-site coherent potential approximation. It does not allow one to take into proper account the local-environment effects, because in this case only a single scatterer is treated exactly. Moreover, the single-site CPA leads to ambiguity

in describing charge-transfer effects in alloys. Nevertheless, as will be shown in this paper, good agreement of the calculated results with experimental data can be obtained by a suitable choice of the Madelung potential of the alloy's components. In Sec. III, we describe the details of our electronic structure calculations for random Al-Li alloys. The calculated electronic structure and the cohesive properies of Al-Li alloys are discussed in Sec. IV. In Sec. V, we present the technique and the results of our calculations of the thermal and elastic properies of Al-Li alloys. Some concluding remarks are made in Sec. VI. In the Appendix, we substantiate the high-temperature relation between the Grüneisen constant and Poisson's ratio for an isotropic solid which we use for thermal property calculations.

II. THE MADELUNG POTENTIAL AND ENERGY OF A COMPLETELY RANDOM ALLOY IN THE SINGLE-SITE CPA

Usually it is accepted that the Madelung potential and energy of a random alloy in the single-site CPA have no additional terms connected with the charge-transfer effects between atoms of different types.[18] This is one of the most doubtful features of the CPA, which as a rule is substantiated by the electroneutrality of a single-site effective medium whose atoms are regarded as equal to one another. However, in a real random alloy any atomic configuration is possible in the underlaying lattice, and consequently, atoms of the same type may have different local atomic environments. In this case, it is obvious that their electronic states and particularly their net charges will also differ. Such fluctuations of the net charge should lead to an additional contribution to the Madelung energy.

Recently, Zunger and co-workers[19,20] have examined this problem with the help of a cluster expansion of electrostatic lattice energy. In their model, the net charge of an atom is proportional to the number of atoms of the unlike type at the first coordination shell. As a consequence, they found that the Madelung energy for binary random alloy was nonzero and it could be written as

$$E_{\mathrm{Mad}}^{\mathrm{dis}} \sim -c(1-c)\lambda^2/R \ . \tag{1}$$

Here c is the concentration of one of the components, R is the nearest-neighbor bond length, and λ is a scaling constant determining the maximum charge transfer when all the nearest-neighboring atoms are of an unlike type.

On the basis of these results, the authors of Ref. 20 have drawn the conclusion that it is impossible to give a correct description of the thermodynamic properties of random alloys with a nonzero charge transfer within the single-site CPA, since the value of $E_{\mathrm{Mad}}^{\mathrm{dis}}$ has the same order of magnitude as the Madelung energy of ordered phases.

In this section we are going to show that in fact the zero Madelung energy in the single-site CPA is not an artifact of the theory but rather a consequence of the model of the Madelung potential of alloy components in the effective medium. The choice of a different model leads to a result analogous to (1) even in the *mean-field approximation*. For the sake of simplicity, we shall consider a simple model of a completely random alloy in the atomic sphere approximation.

Let us assume that charge-transfer effects in a binary random alloy A_cB_{1-c} are formed by the nearest-neighbor interaction between atoms, i.e., the value of a charge coming from atom α to atom β, $q^{\alpha\beta}$, is equal to zero when these atoms are not nearest neighbors. Then the value of the average net charges of the A and B atoms are written as

$$\begin{aligned} \Delta q_A &= [cq^{AA} + (1-c)q^{AB}]Z \ , \\ \Delta q_B &= [cq^{BA} + (1-c)q^{BB}]Z \ , \end{aligned} \tag{2}$$

where Z is a coordination number of the first shell.

We can also determine the average net charge of the A and B atoms which are next to the A atom:

$$\begin{aligned} \Delta q_A^A &= \Delta q_A(Z-1)/Z + q^{AA} \ , \\ \Delta q_B^A &= \Delta q_B(Z-1)/Z + q^{AB} \ . \end{aligned} \tag{3}$$

Then the Madelung potential of the A and B atoms keeps only a term from the first shell and after being averaged in the mean-field approximation it will have the form

$$\begin{aligned} V_{\mathrm{Mad}}^A &= -e^2/RZ\{c[\Delta q_A(Z-1)/Z + q^{AA}] \\ &\quad +(1-c)\Delta q_B(Z-1)/Z + q^{AB})\} \\ &= -\Delta q_A e^2/R \ , \\ V_{\mathrm{Mad}}^B &= -\Delta q_B e^2/R \ . \end{aligned} \tag{4}$$

In order to get expression (4) the condition of electroneutrality: $c\Delta q_A + (1-c)\Delta q_B = 0$ has been taken into account. Thus, in the single-site CPA, by neglecting the interaction of nearest-neighboring atoms between each other, we can write the Madelung energy of an alloy as

$$\begin{aligned} E_{\mathrm{Mad}} &= cV_{\mathrm{Mad}}^A \Delta q_A + (1-c)V_{\mathrm{Mad}}^B \Delta q_B \\ &= -c(1-c)e^2(\Delta q_A - \Delta q_B)^2/R \ . \end{aligned} \tag{5}$$

Expression (5) is very close to result (1), and it can be shown that (5) differs from (1) by a constant factor which, for example, for fcc lattice is equal to 1.521, and it mainly takes into account just the interaction between the nearest neighbors of the impurity.

It is easy to demonstrate that a different choice of the model for the $q^{\alpha\beta}$ leads to a similar result for the Madelung potential and energy. We get zero Madelung potential and energy only if we assume that $q^{\alpha\beta}$ does not depend on the distance between α and β atoms.

Since the potentials of all but the impurity atom itself are excluded from the scheme of the single-site LDA self-consistency, the charge distribution in the effective medium around an impurity atom cannot be ascertained in the single-site CPA. If we assume that the net charge of the alloy components are completely screened by their closest environment, the Madelung potential of the alloy components and the Madelung energy of the alloy are defined by Eqs. (4) and (5). Whereas, the zero Madelung potential and energy in the CPA is true of all atoms of an alloy equally perturbed by any given atom regardless of the distance to it.

From the mathematical point of view, all these models are on an equal footing. Therefore, the choice of a concrete model should be decided after a further physical analysis based on a comparison of the results obtained in these models with the experimental data and/or with the results obtained by more sophisticated methods.

Since this problem originates from the single-site approximation, the best way to solve it is to consider the impurity atom and its environment in a matrix which corresponds to the dilute limit of the alloy. It is obvious that the answer to the problem depends on the nature of the matrix, but for a metal matrix numerous calculations show that the charge density perturbation is small beyond the impurity nearest-neighbor shell and practically the whole net charge of the impurity is compensated for by the net charges of its nearest neighbors.[21,22] It is clear from the physical point of view because the screening radius in metals is about 1–1.5 Å which corresponds to the nearest-neighboring distance between atoms. Thus, taking into account these results and our experience in the calculation of the thermodynamic properties of disordered alloys[23,24] we can conclude that the model of screening by the nearest neighbors is the most adequate for metallic systems in the single-site approximation, and we use it in our LMTO-CPA-LDA calculations in this work.

III. COMPUTATIONAL DETAILS

The self-consistent LMTO-ASA-CPA method was applied to calculate the electronic structure and volume- and concentration-dependent total energies of random Al-Li alloys. The method was previously described in Ref. 16 and 17. The integration of the Green's function over the energy to evaluate moments of the density of electronic states was carried out along the semicircular contour comprising 12 points in the complex plane. The Brillouin zone integration was performed by employing the Weyl uniform **k**-point distribution[25] which enabled us to solve the CPA equations simultaneously with integration. To achieve the necessary convergence of the integral at real values of energy we had to take 1500 points in the irreducible wedge of the Brillouin zone.

The chosen radii of the aluminum and lithium atomic spheres were equal. Angular-momentum truncation was performed at $l_{\max} = 2$, i.e., we took s, p, and d states into account in our calculations. In order to estimate the thermodynamic properties of alloys, we performed six LDA self-consistent calculations with different lattice parameter values for 12 concentrations of the alloys under investigation. The total energies of the pure elements were obtained by the extrapolation of the local Al (Li) total energy contribution to the zero (unity) of the Li concentration. The results of this procedure were verified by the direct total-energy LMTO atomic-sphere approximation (ASA) calculations for pure Al and Li. To eliminate the errors caused by the linear tetrahedron integration method, we extrapolated the LMTO-ASA total energies to the infinitely large number of **k** points in the coordinates E_{tot} vs $n^{-2/3}$.[26] The total energies obtained in both ways differ less than 0.1 mRy. In all calculations the Perdew-Zunger formula[27] for the exchange-correlation potential and energy in the local-density approximation was taken.

IV. ELECTRONIC STRUCTURE AND CHARGE TRANSFER

In Fig. 1 we display total and local DOS in a number of random fcc Al-Li solid solutions and in the Al_3Li compound.[13,14] In contrast to the DOS of Al-rich alloys there are several sharp peaks in the DOS of the Al_3Li compound. By comparing the angular momentum and site-projected DOS in Fig. 2 it is evident that these peaks are caused by strong hybridization. (It is necessary to note that in Ref. 9 the Li-projected DOS turned out to be very small and showed no distinctive features. But we assume that the authors confused the units in determining the Li DOS curve.) For instance, the first peak near −0.6 Ry appears due to the s-p hybridization between Al s and Li p states. The second and the third peaks at −0.4 Ry and −0.3 Ry are correspondingly a consequence of hybridization between Al s and p electrons and p electrons of Li. The group of peaks near the Fermi energy that correspond to Al and Li p states evidently have a different nature. Their proximity to the Fermi energy and the similarity of the Li and Al p-states DOS in

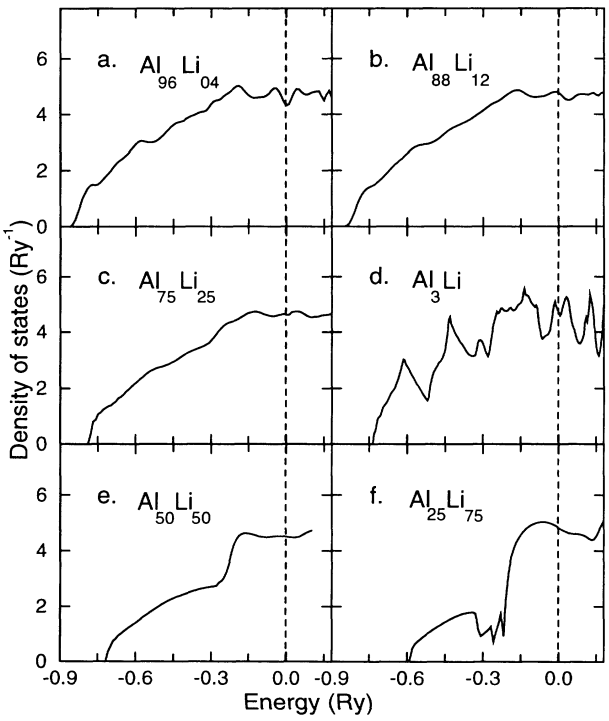

FIG. 1. Density of states for the ordered Al_3Li phase ($L1_2$ structure) and random fcc Al-Li solid solutions. In (a), (b), (c), (e), and (f) are shown the densities of states for $Al_{96}Li_{04}$, $Al_{88}Li_{12}$, $Al_{75}Li_{25}$, $Al_{50}Li_{50}$, and $Al_{25}Li_{75}$ random alloys, respectively, and in (d) for Al_3Li ordered phase. The dashed line designates the Fermi energy of an alloy.

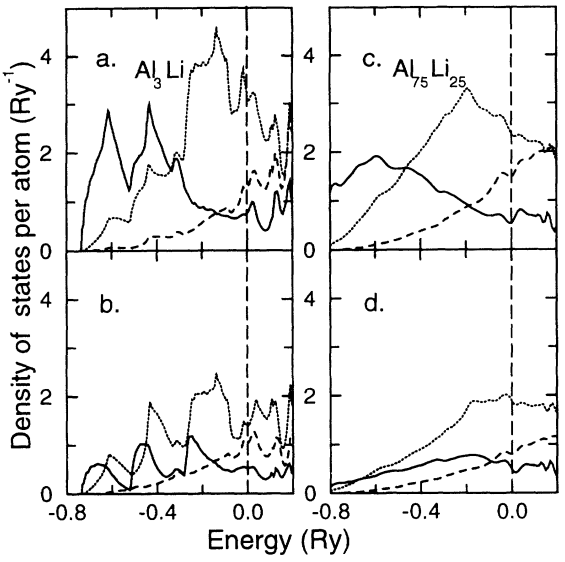

FIG. 2. Partial decomposition of the local densities of states of the ordered Al_3Li phase and disordered $Al_{75}Li_{25}$ alloy. In (a) and (c) are shown the local DOS projected onto Al sites in Al_3Li and $Al_{75}Li_{25}$, respectively, and in (b) and (d) the local DOS projected onto Li sites. The partial s DOS is shown by a solid line, the partial p DOS by a dotted line, and the partial d DOS by a dashed line.

this rather wide region indicate that most probably this part of p states in the Li sphere comes from suitable Al states that dangle into the Li sphere. This is also true of most of the states of Li d character.[9] It is noteworthy that despite the fact that the radius of the Li atomic sphere decreases in Al-rich alloys the number of p and d states in it increases singificantly as is seen from Table I, and they reach their maximum values in the ordered Al_3Li phase where each Li atom is surrounded only by Al atoms.

All distinctive features of the Al_3Li DOS disappear in the DOS of Al-rich random alloys and it is impossible to see any hybridization effects on the partial Al- and Li-projected DOS (Fig. 2). The main factor in this case that leads to the disappearance of the peaks of the DOS is the random character of the alloys. Besides, the single-site CPA can result in the inaccuracy of the description of the hybridization effects. However, the absence of distinctive features in the DOS itself does not mean that there are no hybridization effects.

The DOS of the Li-rich alloys are divided into two distinctive parts. The low-energy part corresponds to the Al $3s$ states which part from the Li valence band when there is Al impurity in the Li matrix.

Now we will go over to the charge-transfer effects in the Al-Li alloys and we will show that they play an important role in the formation of ground-state and thermodynamic properties. Let us return to Table I and Fig. 3. According to the values of the net charges of the Al and Li atomic spheres there is a significant charge transfer from Al to Li atoms in the whole concentration range. Besides, the concentration dependence of the net charges in the atomic spheres is very strong. But as has been shown in Ref. 17 the suitable quantity for the definition of charge transfer in the ASA is an effective charge transfer: $q^* = \Delta q_A - \Delta q_B$. This quantity also appears in expression (5) for the Madelung energy of a random alloy and, therefore, has a transparent physical meaning. For instance, in the linear model for the atomic sphere charges,[20] used for the cluster expansion of Madelung energy, q^* is equal to 24λ, i.e., the maximal charge of the atomic sphere that is surrounded by atoms of an unlike type. If the value of q^* in an alloy does not depend on the concentration, as, for example, in the Ni-Al system,[17] the value of the atomic sphere charge is proportional to the number of the nearest-neighbor atoms of the unlike type, and such a system can be described by the linear model.[19,20]

In Fig. 3, the values of the net charges and the effective charges are presented as a function of the alloy concentration. It is obvious that the effective charges deviate greatly from the constant value, thus the linear model is unacceptable for the Al-Li system. In Fig. 4, we show the Madelung contribution to the total energy of the random Al-Li alloys. As the Madelung energy is proportional to the square of q^*, it has a correspondingly asymmetrical form. But the Madelung energy contributes directly

TABLE I. Total and partial occupation numbers of valence electrons in the atomic spheres of random Al-Li alloys, pure fcc Al and Li, and the Al_3Li ordered phase ($L1_2$).

	Al				Li				
Alloy	Total	s	p	d	Total	s	p	d	R_{WS} (a.u.)
Al	3.0	1.079	1.495	0.426					2.95
$Al_{96}Li_{04}$	2.981	1.074	1.492	0.415	1.467	0.424	0.811	0.232	2.95
$Al_{88}Li_{12}$	2.943	1.089	1.478	0.367	1.416	0.422	0.785	0.209	2.95
$Al_{75}Li_{25}$	2.886	1.110	1.458	0.318	1.342	0.419	0.747	0.176	2.95
Al_3Li	2.824	1.102	1.454	0.268	1.530	0.429	0.849	0.252	2.95
$Al_{50}Li_{50}$	2.801	1.158	1.429	0.214	1.199	0.416	0.663	0.120	2.99
$Al_{25}Li_{75}$	2.767	1.222	1.421	0.124	1.078	0.446	0.561	0.071	3.07
$Al_{12}Li_{88}$	2.774	1.253	1.435	0.086	1.031	0.471	0.510	0.050	3.11
$Al_{04}Li_{96}$	2.826	1.305	1.457	0.064	1.007	0.497	0.473	0.037	3.21
Li					1.0	0.504	0.464	0.032	3.25

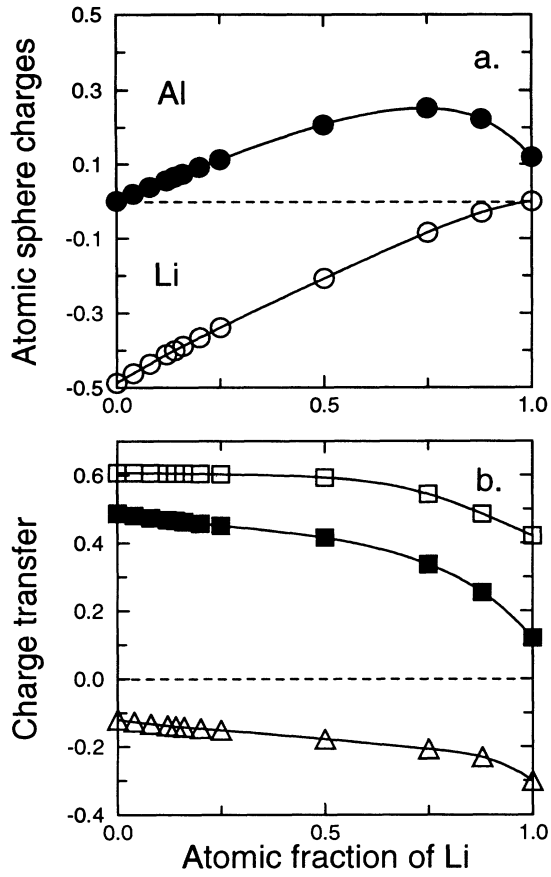

FIG. 3. Atomic sphere net charges (a) and charge transfer (b) in Al-Li alloys. In (a) the net charge of the Al atomic sphere is shown by closed circles and the net charge of the Li atomic sphere by open circles. In (b) open squares show the effective charge transfer q^*_{OCD} obtained in the OCD model and closed squares show the effective charge transfer q^*_{SC} after self-consistent LDA calculation. "True" charge transfer, which can be defined as their difference $\Delta q = q^*_{\mathrm{SC}} - q^*_{\mathrm{OCD}}$, is shown by open triangles.

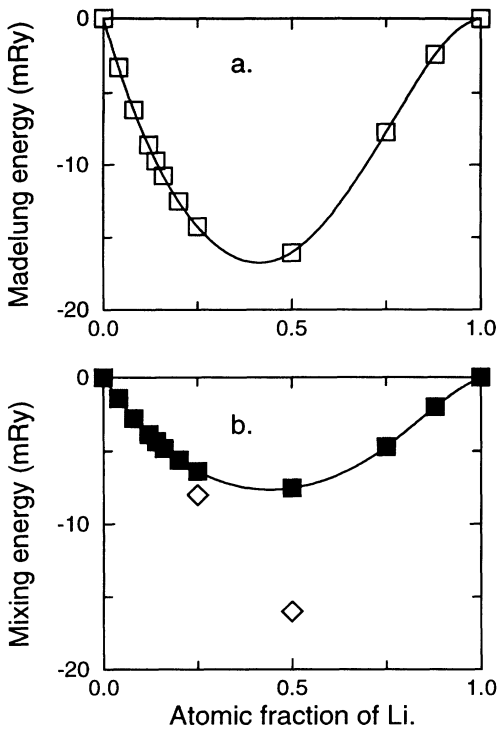

FIG. 4. The Madelung energy (a) and the mixing energy (b) of the random fcc Al-Li alloys. Closed squares in (b) show the results of the calculation for random alloys and open diamonds designate the enthalpies of formation of Al_3Li ($L1_2$) and AlLi ($B32$) ordered phases obtained in the FLAPW calculations (Ref. 9).

to the mixing enthalpy, and therefore, as is seen in Fig. 4, the mixing enthalpy curve has a form analogous to the curve of the Madelung energy. The mixing enthalpy is negative and its value is in agreement with the enthalpies of the formation of the ordered Al_3Li and LiAl compounds.[9]

Madelung energy also strongly influences the ground-state properties because the value of the effective charge transfer q^* is very sensitive to the Wigner-Seitz radius S, and the smaller the S, the greater the q^*. Hence, the Madelung contribution to the total energy must lead to the shortening of the equilibrium lattice parameter. Therefore, the obtained decrease of the charge transfer in the Li-rich part corresponds to a strong increase of the equilibrium lattice parameter of alloys containing more than 50 at. % of lithium (Fig. 5). It is noteworthy that our calculations, carried out within the standard scheme without regard to the Madelung contribution to the one-electron potential and total energy, result in producing positive values of the mixing enthalpies in the whole concentration range and conform to Vegard's law for the lattice parameters.

As a matter of fact, q^* cannot be regarded as a quantity that really describes the charge transfer, caused by the distinction of the electronegativities of the different atoms. For example, the division of the crystal into atomic spheres is an artificial procedure, and the value of q^* greatly depends on the choice of the ratio of the radii of atomic spheres. To define a "true" charge transfer it is necessary to choose a reference state in order to compare

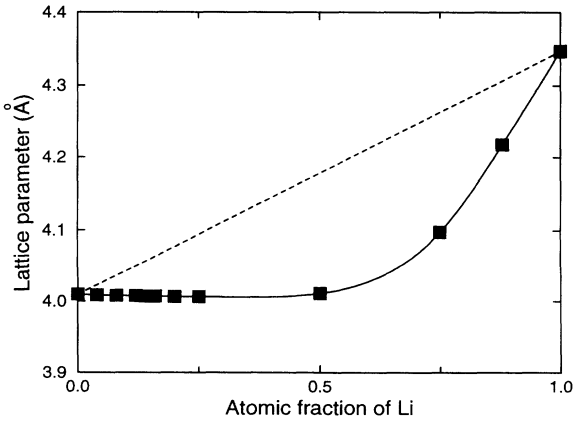

FIG. 5. Calculated concentration dependence of the lattice parameter of Al-Li random alloys at 0 K.

the value of q^* after an LDA self-consistent calculation and q^* in a state when the chemical interaction of elements is not taken into account. Such a state can be determined by the overlapping charge densities (OCD) model. In this way we can define the charge transfer as $\Delta q = q^*_{SC} - q^*_{OCD}$, where q^*_{SC} and q^*_{OCD} are effective charge transfers, obtained, respectively, within the LDA self-consistent calculations and the OCD model. The concentration dependencies of the q^*_{OCD}, q^*_{SC}, and Δq are also shown in Fig. 3. The absolute value of Δq turns out to be smaller than that of q^*, and its sign is the opposite of the sign q^*, which corresponds to the charge transfer from Li to Al atoms in accordance to their electronegativities.

V. THERMAL AND ELASTIC PROPERTIES

The thermal and elastic properties of Al-Li alloys are of great interest. Actually, the direct first-principle calculations of both of these properties are impossible in the atomic sphere approximation, which does not allow one to obtain the correct values of the energy of any anisotropic deformation of solids. However, Moruzzi *et al.*[28] have shown that the thermal properties of most cubic metals can be estimated in the Debye-Grüneisen model with good accuracy only from the binding curves, i.e., without calculations of anisotropic deformations. In this section, we introduce a simple ansatz which for isotropic solids in the high-temperature limit makes the model described in Ref. 28 more accurate and enables one to calculate their elastic properties only on the basis of binding curve data as well.

Two parameters are sufficient to evalute the vibrational contribution to the Helmholtz free energy in the Debye-Grüneisen model: a characteristic Debye temperature Θ_D and a Grüneisen constant γ. Moruzzi *et. al.*[28] suggested the following simple expressions for their determination:

$$\gamma = -1 - \frac{V}{2}\frac{\partial^3 E/\partial V^3}{\partial^2 E/\partial V^2}, \tag{6}$$

$$\Theta_D = h/k_B \left[\frac{3}{4\pi\Omega}\right]^{1/3} \bar{v}, \tag{7}$$

where E is the total energy of a solid, h and k_B are Planck's and Boltzmann's constants, V is its atomic volume, and $\bar{v}$ is the mean sound velocity in the solid. The latter can be expressed in the form

$$\bar{v} = C\left[\frac{B}{\rho}\right]^{1/2}, \tag{8}$$

where ρ is the density of a solid, B is the bulk modulus, and C is the dimensionless coefficient

$$C = \left[\frac{1}{3}(L/B)^{-3/2} + \frac{2}{3}(G/B)^{-3/2}\right]^{-1/3}. \tag{9}$$

Here L and G are longitudinal and shear moduli, which can be expressed via bulk modulus and Poisson's ratio σ as

$$(L/B) = \frac{3(1-\sigma)}{1+\sigma}, \quad (G/B) = \frac{3(1-2\sigma)}{2(1+\sigma)}. \tag{10}$$

Thus, it follows that to calculate the thermal properties it is necessary to know either the relation between L and G or Poisson's ratio. As both these parameters are almost constant for a number of pure cubic metals, Moruzzi *et al.*[28] suggested that Poisson's ratio is constant and approximately equal to 1/3.

Although both aluminum and lithium are good metals, unfortunately this approximation cannot be used for Al-Li alloys because experiment[2] and pseudopotential calculations[14] show that Poisson's ratio of the Al-Li solid solutions vary with the Li concentration. Therefore, to analyze the concentration dependencies of the thermal properties of Al-Li random alloys one should take the corresponding concentration dependence of Poisson's ratio into account. For this purpose we utilize the following high-temperature relation for isotropic elastic medium between Poisson's ratio and the Grüneisen constant (its derivation is given in the Appendix):

$$\sigma = \frac{4\gamma - 3}{6\gamma + 3}. \tag{11}$$

The calculated concentration dependencies of γ, σ, and $(\Theta_D)_0$ for the Al-rich alloys are shown in Fig. 6. It is

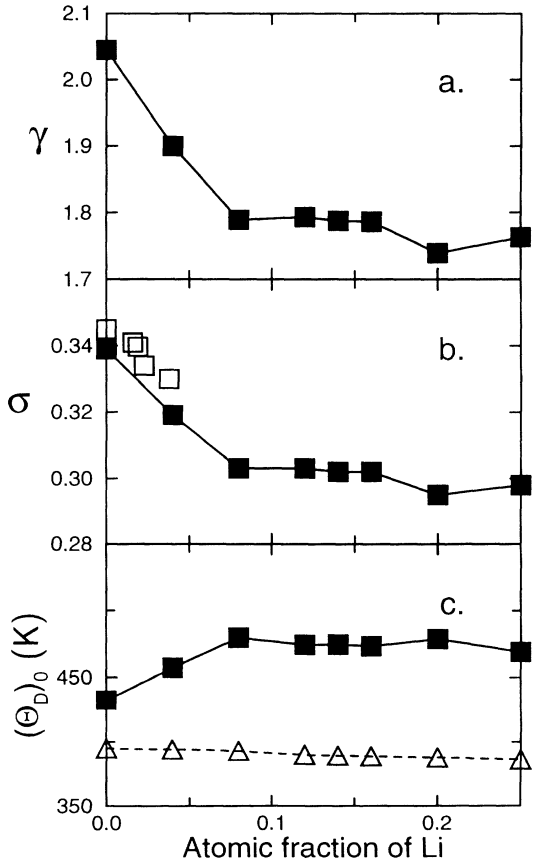

FIG. 6. The Grüneisen constant (a), Poisson's ratio (b), and Debye temperature (c) of Al-rich Al-Li alloys. Closed squares are the results of the calculation and open squares show experimental data for Poisson's ratio (Ref. 2). In (c), open triangles show the Debye temperature calculated by means of the formulas suggested in Ref. 28.

noteworthy, that our estimation of Poisson's ratio yields its value and concentration dependence in good agreement with the experimental ones.[2] In contrast to our results, the Debye temperature obtained by means of the formulas of work[28] decreases with the Li addition. However, the Debye temperature experimental measurements for Li-contained alloys show a growth of Θ_D with the Li addition.[29] In this connection we believe that our method of Debye temperature estimation is more reliable in regard to alloys.

The simple relation between γ and σ enables us to estimate the values of the room-temperature Young's modulus E and shear modulus G for the alloys under consideration on the basis of binding energy curves data alone (see the Appendix). Figures 7 and 8 present the calculated and experimental room-temperature properties of the Al-rich alloys as functions of alloy concentrations. It is obvious that the increase of E and G values at a small concentration of Li is connected with the decrease of the Grüneisen constant and, respectively, Poisson's ratio. When the concentration of Li in an alloy exceeds 4–8 at. %, the Grüneisen constant becomes a weak concentration dependent, and the values of E and G moduli are mostly determined by the bulk modulus decrease. This anomaly may be related to the topological phase transition,[30] but in the present work we do not analyze the thermal property trends in the vicinity of possible topological phase transition points in any detail. Our calculations also predict the decrease of the lattice parameter and bulk modulus for the Al-rich alloys with Li addition. Unfortunately, we can compare these properties with experimental data[2,3] only for small concentrations of Li ($\leq$ 4 at. %) which are true of homogeneous solid solutions. But in this region the agreement between our results and the experimental data is very good.

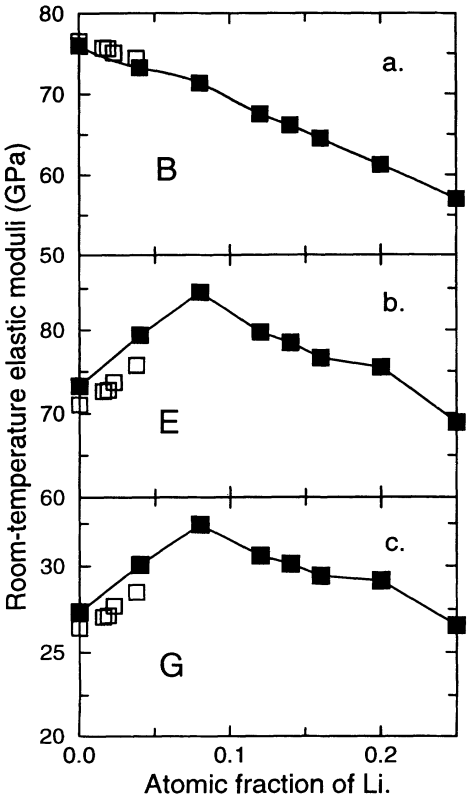

FIG. 7. The room-temperature bulk (a), Young's (b), and shear (c) moduli of Al-rich Al-Li alloys. Closed squares show the calculated results and open squares correspond to experimental data (Ref. 2).

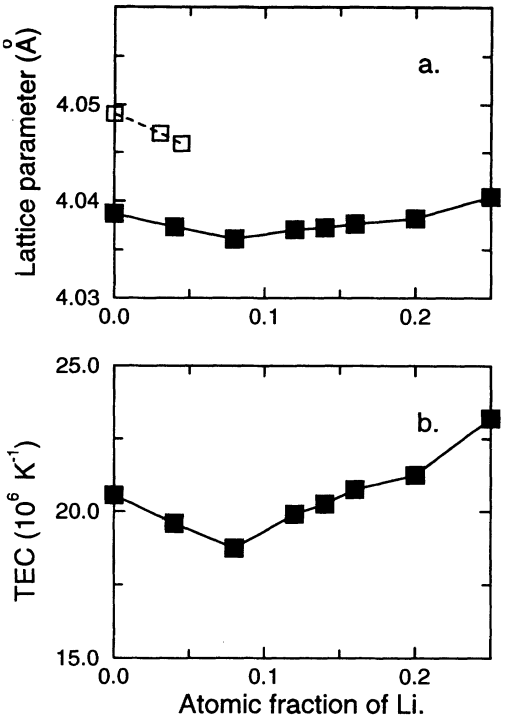

FIG. 8. The room-temperature lattice parameter (a) and thermal expansion coefficient (TEC) (b) of the Al-rich Al-Li alloys. The calculated results are shown by closed squares and experimental data (Ref. 3) by open squares.

In the Helmholtz free energy calculations we followed Refs. 17 and 28 in which the details of such calculations were described. The calculated concentration dependence of the room-temperature thermal expansion coefficient (TEC) of Al-Li random alloys is also shown in Fig. 8. Our calculations predict the decrease of the TEC value at small concentrations of Li. Unfortunately, we do not know of any reliable experiments in regard to the influence of Li alloying on the thermal expansion of aluminum-based alloys.

VI. SUMMARY

This paper reports the implementation of a self-consistent coherent potential technique to calculate the electronic structure, thermodynamic, and thermal properties of random Al-Li alloys. In order to overcome the ambiguity induced by the single-site CPA in the definition of the Madelung potential and energy, we propose a simple physical approach. Our approach leads to a significant contribution to the one-electron potential of the alloy components and correspondingly to the total energy of the alloy when the net charges of its compo-

nents differ from each other. We show that the screening model for the Madelung potential and energy plays an important role by obtaining the correct thermodynamic and ground-state properties of an alloy. For example, we managed to obtain reasonable values of the mixing enthalpies and a strong negative deviation of the lattice parameters from Vegard's law only due to the screening Madelung potential.

In order to compare the calculated thermodynamic properties with the experimental ones at finite temperatures, we took into account the phonon contribution to the free energy of an alloy in the Debye-Grüneisen model. To make this model free of empirical parameters we derived and employed a heuristic formula connecting the Grüneisen constant with Poisson's ratio. As a result we obtained bulk, Young's and shear moduli, and the coefficients of thermal expansion at room temperature which are in good agreement with available experimental data.

ACKNOWLEDGMENTS

One of us, A.V.R, would like to thank Professor B. Johansson and his group for their hospitality at the Uppsala University, where the final version of this paper was prepared. We are also very grateful to Dr. I. A. Abrikosov for his constant interest in this work and our helpful discussions.

APPENDIX: HIGH-TEMPERATURE RELATION BETWEEN THE GRÜNEISEN CONSTANT AND POISSON'S RATIO

The main idea of the following derivation belongs to Leontyev.[31] Let us consider an elastically isotropic solid with volume V at temperature T. Temperature T is assumed not to be lower than the characteristic Debye temperature Θ_D of the actual solid (the classical limit).

These assumptions allow us to express the kinetic energy density of thermal vibrations in terms of weight density ρ and the mean-square velocity of atomic displacements $\bar{v}^2$. The internal energy U of the isolated solid, evoked by thermal vibrations, is a total differential with respect to variables T and V:

$$\left(\frac{\partial U}{\partial T}\right)_V dT + \left(\frac{\partial U}{\partial V}\right)_T dV = 0. \tag{A1}$$

Using the well-known thermodynamic identities

$$\left(\frac{\partial U}{\partial T}\right)_V = C_V\ ,$$
$$\left[\left(\frac{\partial U}{\partial V}\right)_T + P\right]\left(\frac{\partial V}{\partial T}\right)_P = C_P - C_V, \tag{A2}$$

together with the following definition of the bulk thermal expansion coefficient:

$$\beta = \frac{1}{V}\left(\frac{\partial V}{\partial T}\right)_P\ , \tag{A3}$$

(A1) can be rewritten as:

$$PV = \frac{C_P}{\beta}. \tag{A4}$$

Here P is the internal pressure, caused by thermal vibrations, C_P and C_V are heat capacities at constant pressure and volume, respectively. According to the virial theorem, we can write P as $P = \frac{2}{3}\rho\bar{v}^2$ and, consequently,

$$\rho\bar{v}^2 = \frac{3}{2}\frac{C_P}{\beta V}. \tag{A5}$$

Regarding the thermal vibrations as a superposition of standing waves and in the classical limit we can give

$$\rho\bar{v}^2 = \frac{1}{3}(L_a + 2G_a) = B_a\left(\frac{2-3\sigma}{1+\sigma}\right). \tag{A6}$$

Here L_a, G_a, and B_a are adiabatic longitudinal, transversal, and bulk elastic moduli, respectively, and σ is the Poisson's ratio.

By equating the right sides of (A5) and (A6) and taking into account the definition of the Grüneisen constant,

$$\gamma = \frac{\beta B_a V}{C_P}, \tag{A7}$$

we obtain

$$\sigma = \frac{4\gamma - 3}{6\gamma + 3}. \tag{A8}$$

Now we will illustrate how relation (A8) works in real systems. Let us consider cubic crystals with central and pairwise interatomic forces. In this case the Cauchi relation $c_{12} = c_{44}$ is fulfilled, and hence taking into account that

$$c_{12} = 3\frac{\sigma}{1+\sigma}B,\quad c_{44} = \frac{3}{2}\frac{1-2\sigma}{1+\sigma}B, \tag{A9}$$

it follows that for such a crystal at high temperature, Poisson's ratio must be equal to 0.25, and the Grüneisen constant, $\gamma = 1.5$, in accordance with (A8). Indeed, the room-temperature Grüneisen constants of alkaline-haloid crystals, e.g., NaCl, KCl, KBr, KI, and LiF, whose strong electrostatic interatomic interaction can be considered as pairwise and central, is very close to the above mentioned value.[32] Formula (A8) leads to quite reasonable results for such systems whose anisotropic coefficient does not appreciably differ from 1. We can also use Eq. (A5) to estimate the Grüneisen constant for an incompressible metal having Poisson's ratio close to 1/3: it is close to 2, as is true of pure Al. As to aluminum and Al-rich Al-Li alloys, they are almost elastically isotropic,[2] and there is no doubt of the applicability of Eq. (A8) in this case.

[1] E. G. Lavernia and N. J. Grant, J. Mater. Sci. **22**, 1521 (1987).

[2] W. Müller, E. Bubeck, and V. Gerold, in *Proceedings of the 3rd International Conference on Aluminum-Lithium Alloys*, edited by C. Baker, P. J. Gregson, S. J. Harris, and C. J. Peel (TMS-AIME, London, 1986), p. 435.

[3] S. H. Kellington, D. Loveridge, and J. M. Titman, Br. J. Appl. Phys. (J. Phys. D) Ser.2 **2**, 1162 (1969).

[4]A. Zunger, Phys. Rev. B **17**, 2582 (1978).
[5]T. Asada, T. Jarlborg, and A. J. Freeman, Phys. Rev. B **24**, 510 (1981).
[6]R. Podloucky, H. J. F. Jansen, X.-Q. Guo, and A. J. Freeman, Phys. Rev. B **37**, 5478 (1988).
[7]K. Masuda-Jindo and K. Terakura, Phys. Rev. B **39**, 7509 (1989).
[8]X.-Q. Guo, R. Podloucky, and A. J. Freeman, Phys. Rev. B **40**, 2793 (1989).
[9]X.-Q. Guo, R. Podloucky, J.-H. Xu, and A. J. Freeman, Phys. Rev. B **41**, 12 432 (1990).
[10]M. Sluiter, D. de Fontaine, X.-Q. Guo, R. Podloucky, and A. J. Freeman, Phys. Rev. B **42**, 10 460 (1990).
[11]D. Lu and A. E. Carlsson, Phys. Rev. B **40**, 980 (1990).
[12]A. V. Ruban and P. A. Korzhavyi, Dok. Akad. Nauk SSSR **314**, 1121 (1990) [Sov. Phys. Dokl. **35**, 891 (1990)].
[13]Yu. H. Vekilov, P. A. Korzhavyi, and A. V. Ruban, Fiz. Tverd. Tela Leningrad **33**, 2480 (1991) [Sov. Phys. Solid State **33**, 1398 (1991)].
[14]V. G. Vaks and N. E. Zein, J. Phys. Condens. Matter **2**, 5919 (1990).
[15]M. J. Mehl, Phys. Rev. B **47**, 2493 (1993).
[16]I. A. Abrikosov, Yu. H. Vekilov, and A. V. Ruban, Phys. Lett. A **154**, 407 (1991).
[17]I. A. Abrikosov, A. V. Ruban, D. Ya. Kats, and Yu. H. Vekilov, J. Phys. Condens. Matter **5**, 1271 (1993).
[18]D. D. Johnson, D. M. Nicholson, F. J. Pinski, B. L. Gyorffy, and G. M. Stocks, Phys. Rev. Lett. **56**, 2088 (1986); Phys. Rev. B **41**, 9701 (1990).
[19]R. Magri, S.-H. Wei, and A. Zunger, Phys. Rev. B **42**, 11 388 (1990).
[20]Z. W. Lu, S.-H. Wei, A. Zunger, S. Frota-Pessoa, and L. G. Ferreira, Phys. Rev. B **44**, 512 (1991).
[21]R. Zeller, J. Phys. **17**, 2123 (1987).
[22]N. Stefanou, R. Zeller, and P. H. Dederichs, Phys. Rev. B **35**, 2705 (1987).
[23]I. A. Abrikosov, Yu. H. Vekilov, P. A. Korzhavyi, A. V. Ruban, and L. E. Shilkrot, Solid State Commun. **83**, 867 (1992).
[24]S. I. Simak, A. V. Ruban, and Yu. H. Vekilov, Solid State Commun. **87**, 393 (1993).
[25]H. Akai, J. Phys. Condens. Matter **1**, 8045 (1989).
[26]H. J. F. Jansen and A. J. Freeman, Phys. Rev. B **30**, 561 (1984).
[27]J. P. Perdew and A. Zunger, Phys. Rev. B **23**, 5048 (1981).
[28]V. L. Moruzzi, J. F. Janak, and K. Schwarz, Phys. Rev. B **37**, 790 (1988).
[29]A. G. Fox and R. M Fisher, J. Mater. Sci. Lett. **7**, 301 (1988).
[30]V. G. Vaks and A. V. Trefilov, J. Phys. F **18**, 213 (1988).
[31]K. L. Leontyev, Akust. Zh. **XXVII**, 554 (1981).
[32]G. K. White, Proc. R. Soc. London, Ser. A **286**, 204 (1965).